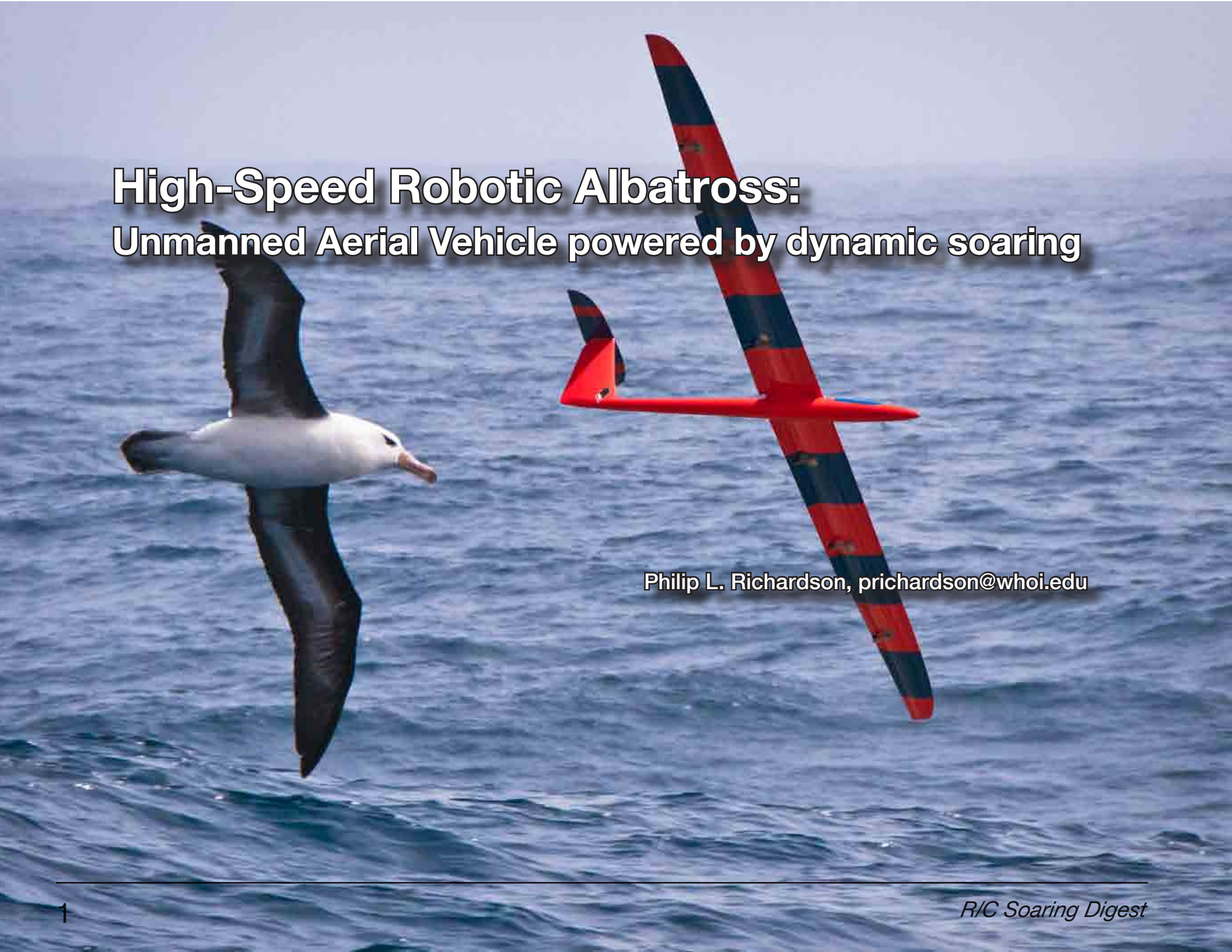

High-Speed Robotic Albatross:

Unmanned Aerial Vehicle powered by dynamic soaring

Philip L. Richardson, prichardson@whoi.edu

Abstract

Wandering albatrosses exploit the vertical gradient of wind velocity (wind shear) above the ocean to gain energy for long distance dynamic soaring with a typical airspeed of 36 mph. In principle, albatrosses could soar much faster than this in sufficient wind, but the limited strength of their wings prevents a much faster airspeed. Recently, pilots of radio-controlled (RC) gliders have exploited the wind shear associated with winds blowing over mountain ridges to achieve very fast glider speeds, reaching a record of 498 mph in March 2012. A relatively simple two-layer model of dynamic soaring predicts maximum glider airspeed to be around 10 times the wind speed of the upper layer (assuming zero wind speed in the lower layer). This indicates that a glider could soar with an airspeed of around 200 mph in a wind speed of 20 mph, much faster than an albatross. It is proposed that recent high-performance RC gliders and their pilots' expertise could be used to develop a high-speed robotic albatross UAV (Unmanned Aerial Vehicle), which could soar over the ocean like an albatross, but much faster than the bird. This UAV could be used for various purposes such as surveillance, search and rescue, and environmental monitoring. A first step is for pilots of RC gliders to demonstrate high-speed dynamic soaring over the ocean in realistic winds and waves.

1. Introduction

Wandering albatrosses exploit the vertical gradient of wind velocity to fly long distances over the Southern Ocean without flapping their wings in what is called dynamic soaring. The birds' typical cruise velocity through the air is around 36 mph. Given sufficient wind speeds an albatross could use dynamic soaring to fly much faster than 36 mph, but high speeds can cause excessive forces on the bird's wings. The limited strength of the bird's wings prevents them from high-speed dynamic soaring.

Pilots of radio-controlled (RC) gliders exploit fast wind blowing over mountain ridges and use dynamic soaring to fly at very high speeds, reaching a record of 498 mph in March 2012. These high speeds require very strong high-performance gliders and accurate control by the pilots. Accelerations of the gliders reach around 100 times gravity (or more). The fast speeds and strong gliders suggest that the technology of these gliders and the experience of the pilots could be used to help develop a high-speed dynamic-soaring robotic albatross UAV (Unmanned Aerial Vehicle) for flight over the ocean. Such a UAV could be useful for various applications such as surveillance, search and rescue, and remote sampling of the marine boundary layer and ocean surface.

Recently, I developed a simple two-layer model of dynamic soaring to help understand how albatrosses use this technique to soar over ocean waves (Richardson, 2011). This model also provides insight into the characteristics of the much faster RC glider flight, which is more than ten times the typical albatross airspeed (Richardson, 2012). The model provides a framework for evaluating whether high-speed dynamic soaring could be exploited over the ocean.

The following describes the observed dynamic soaring of albatrosses and RC gliders and interprets their flight using the two-layer model. The possibility of high-speed dynamic soaring over ocean waves is discussed. It is concluded that a high-speed robotic albatross UAV is possible given sufficiently large wind and waves, but that this concept needs to be proved by having experienced pilots of RC gliders successfully fly them over the ocean using dynamic soaring.

< *Title page illustration: Conceptual illustration of a robotic albatross UAV soaring over the ocean. An image of a Kinetic 100 RC glider being flown by Spencer Lisenby at Weldon Hill California was superimposed on a photo of a black-browed albatross soaring over the Southern Ocean. Photos by Phil Richardson*

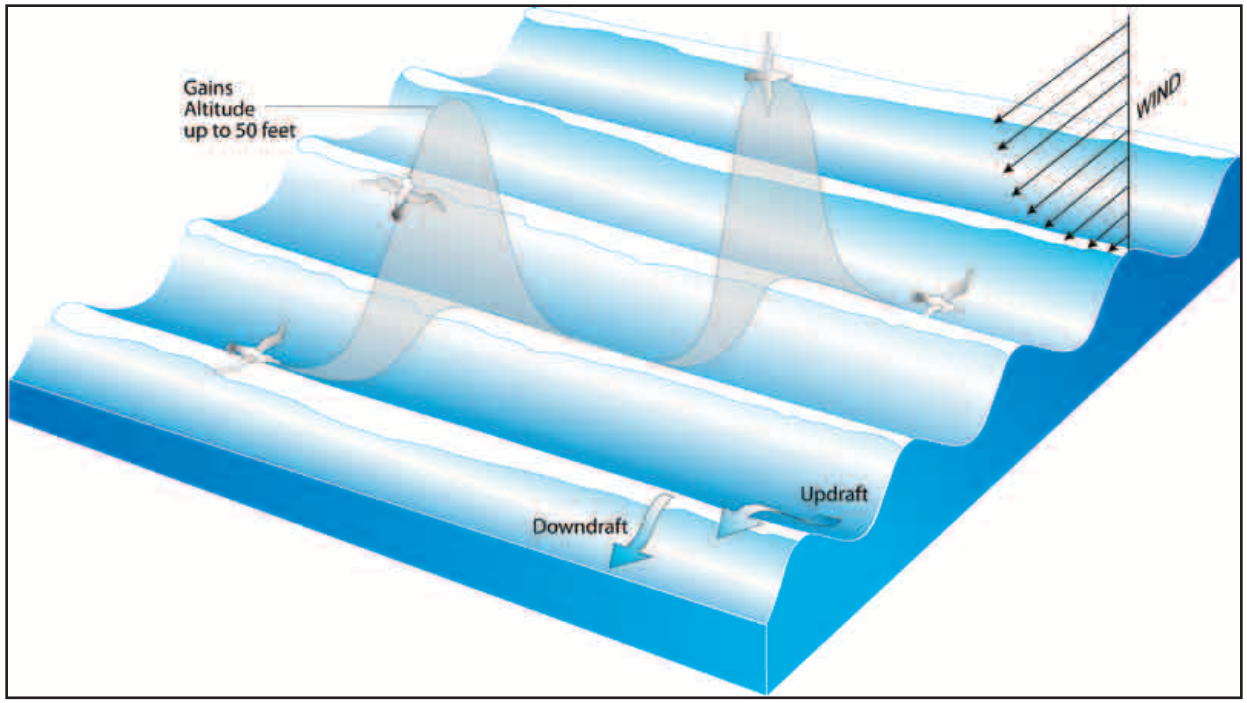

Figure 1. Schematic summary of the zigzag swooping flight pattern of an albatross soaring over waves as observed during a cruise to the South Atlantic. The swooping motion is shown relative to the waves, which are moving downwind. Each climb is upwind and each descent is downwind since the waves are going downwind, although the downwind component is difficult to show in the figure and looks almost parallel to the wave crest. The average direction of flight has an upwind component. The schematic waves are uniform for simplicity; real ocean waves are much more complicated. Regions of updraft and downdraft due to wind blowing over waves are indicated schematically. Simplified vectors of a typical average wind velocity profile over the ocean surface are indicated in the right part of the figure. Most of the vertical gradient of wind velocity (wind shear) is located in a thin boundary layer near the ocean surface. The wave phase speed was not subtracted from the wind speed in this diagram.

2. Albatross soaring over the ocean

I observed wandering albatrosses soaring during two cruises to the South Atlantic. The albatrosses flew in a characteristic and distinctive flight pattern consisting of a swooping motion where each swoop tended to be tightly coupled to a wave crest (Figure 1). Each swoop began with a fast flight parallel to and just above the windward side of a wave. This was followed a turn into the wind and a climb of around 30-50 feet, followed by a downwind descent towards another wave and a turn parallel to the wave. The typical time to complete a swoop was around 10 s. These observations are largely in accord with previous studies (Alerstam et al., 1993; Idrac, 1925, 1931; Pennycuick, 1982).

Figure 1 illustrates an albatross soaring in an upwind direction (as observed) as the bird flew parallel to the ship, which was steaming in a general upwind direction at 12 knots. Of course, albatrosses can soar in other directions too. The observed zigzag snaking flight pattern illustrates the way an albatross extracts energy from the wind using dynamic soaring and uses it to travel over the ocean. Albatrosses can also remain in a particular region by flying in circles or figure-eight patterns.

Dynamic soaring exploits the vertical gradient of wind velocity over ocean waves. The largest vertical gradient of

wind velocity (largest wind shear) is located in a thin boundary layer located within several feet of the water surface. However, the structure of the wind field near the ocean surface is complicated by the presence of waves. Strong wind flowing over a sharp-crested and breaking wave separates from the wave crest forming an area of weaker wind or a lee eddy just downwind of the wave crest (Figure 2) as described by Pennycuick (2002) (see also Gent and Taylor, 1977; Hsu et al., 1981; Kawaii, 1982; Reul et al., 1999). Located above this region of weaker wind is a thin wind-shear region, a wind-shear boundary layer that separates from the upwind wave crest, and above that a layer of stronger wind and reduced wind shear. Pennycuick (2002) proposed that albatrosses take advantage of the strong wind shear located between these two layers downwind of sharp-crested waves in order to gain energy from the wind in what he calls "gust soaring," which is a special case of more general dynamic soaring. Pennycuick (2002) uses the term to mean the rapid increase of wind speed encountered by a bird as it climbs across the thin wind-shear layer located above a lee eddy.

Gust soaring can be understood by using a two-layer approximation first described by Rayleigh (1883) in which a lower layer has zero wind speed and an upper layer has a uniform wind speed of 10 mph (for

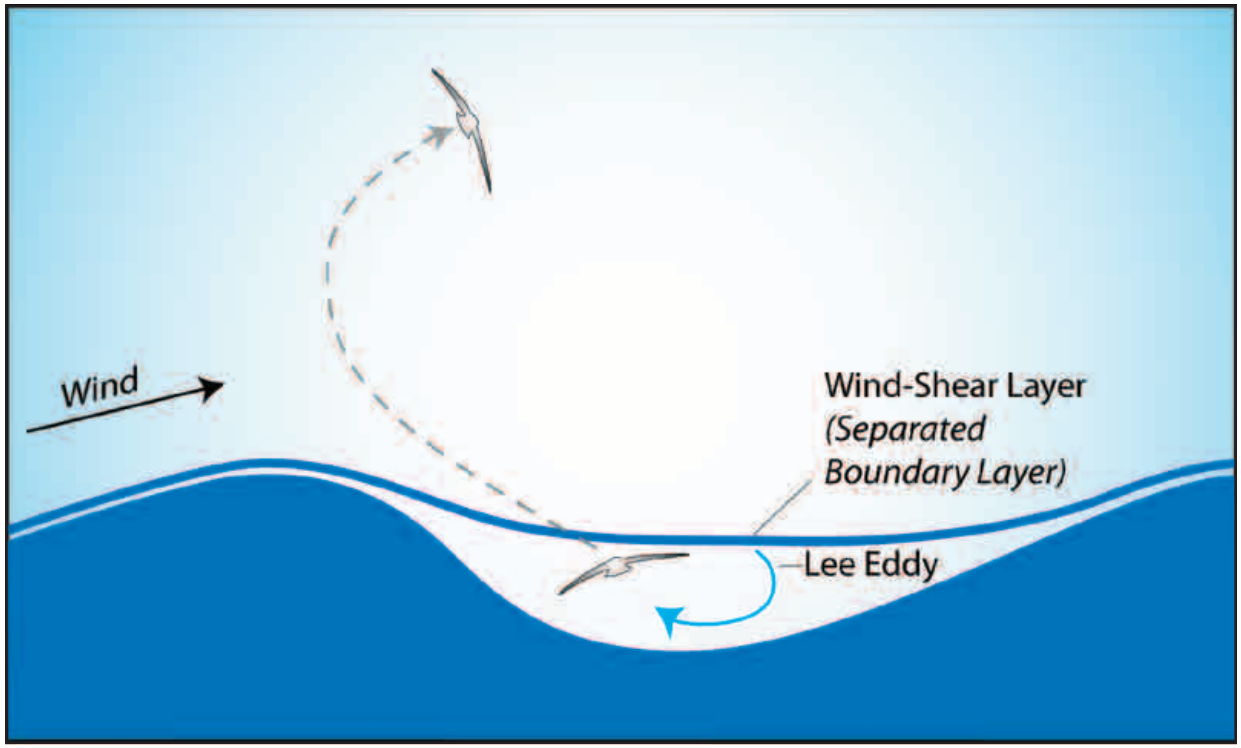

Figure 2. Schematic of an albatross "gust soaring" (after Pennycuick, 2002). Starting in a lee eddy (or separation bubble) located downwind of a sharp-crested wave a bird climbs up through a thin wind-shear layer (separated boundary layer) that has detached from the wave crest. On crossing the wind-shear layer, the bird's airspeed abruptly increases, and the bird experiences a "gust." The increase in airspeed can be used to climb up to heights of 30-50 feet by trading airspeed (kinetic energy) for height (potential energy). A lee eddy is a region of closed streamlines with clockwise circulation in this figure.

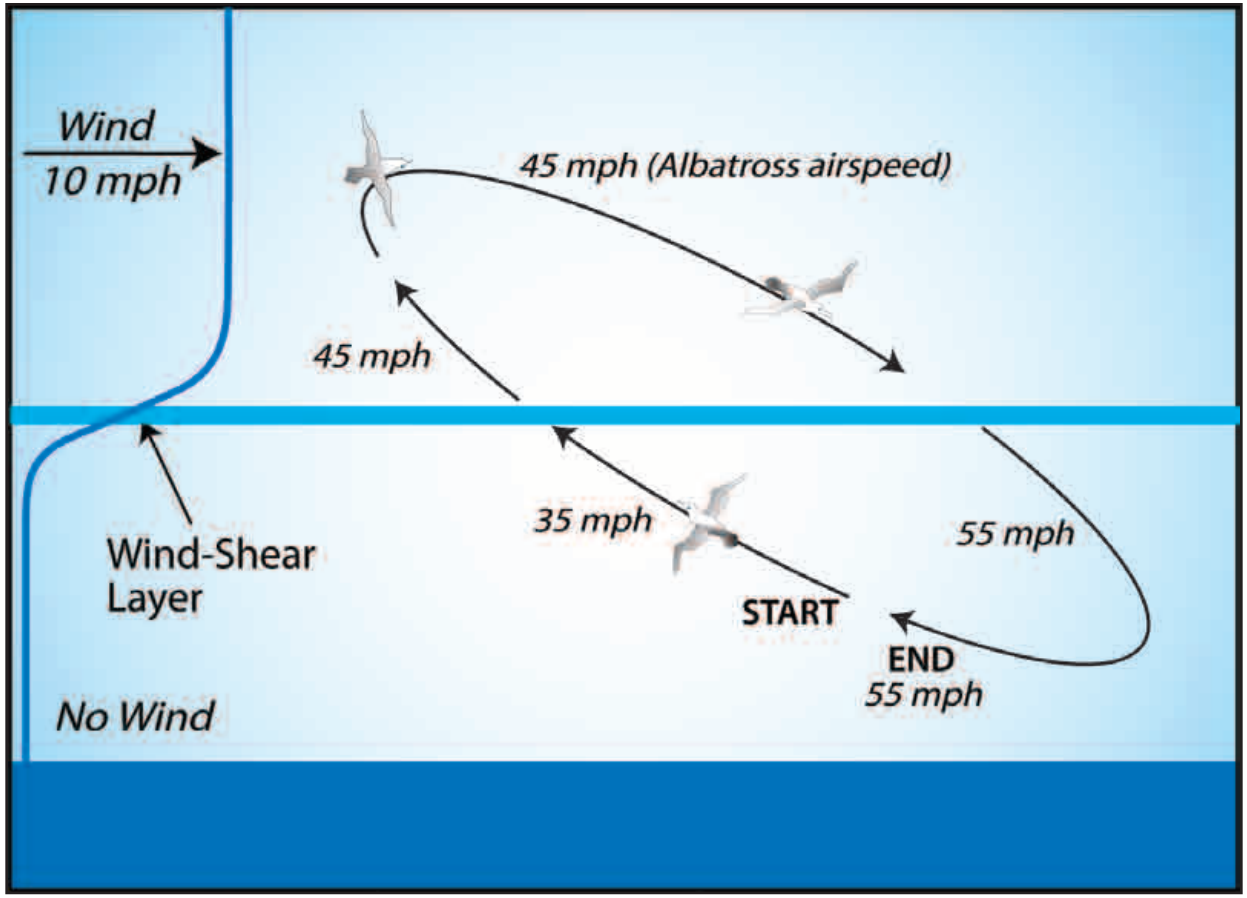

Figure 3. Idealized example of the airspeeds of a dragless albatross gust soaring through a thin wind-shear layer in which the wind increases from zero below the layer to 10 mph above. This example shows how an albatross could gust soar in the region downwind of a wave crest as indicated in Figure 2. Starting in the lower layer with an airspeed of 35 mph an albatross climbs upwind a short distance vertically across the wind-shear layer, which increases the airspeed to 45 mph. The bird then turns and flies downwind with the same airspeed of 45 mph. During the turn, the bird's ground speed increases to 55 mph in the downwind direction and consists of the 45 mph airspeed plus (tail) wind speed of 10 mph. The albatross descends downwind a short distance vertically across the wind-shear layer, which increases airspeed to 55 mph. The bird then turns upwind flying with an airspeed of 55 mph.

example) (Figure 3). A dragless albatross flying at a typical airspeed of 35 mph in an upwind direction in the lower layer pulls up a short distance into the upper layer encountering a 10 mph "gust," which increases the bird's airspeed to 45 mph and adds a pulse of kinetic energy. The bird then turns downwind to fly in the opposite direction and descends into the lower layer, which increases the bird's airspeed to 55 mph, adding another pulse of airspeed and kinetic energy. Thus, in one loop the bird's airspeed increases from 35 mph to 55 mph or two times the 10 mph wind speed of the upper layer. When the energy gained by crossing the wind-shear layer just balances the decrease of energy due to drag, the bird could continuously soar in energy-neutral flight.

The interaction between wind and waves is complicated and depends on the wind velocity and the wave phase velocity. In general the interaction results in a lee eddy or region of closed streamlines synchronous with the wave and located in its trough (Hristov, et al., 2003; Sullivan et al., 2000). A lee eddy can deflect the layer of fast wind away from the wave surface as shown schematically by Figure 2. The upwind part of a lee eddy contains a region of updraft caused partly by the upward orbital motion of the wave surface. This updraft can merge with an updraft due to the wind blowing over the windward wave slope, and the

merged region of updraft can extend above a wave crest (Hristov, et al., 2003; Sullivan, et al., 2000, 2008). An albatross could use the updrafts over waves to gain altitude (potential energy) from the wind in addition to gaining airspeed (kinetic energy) from the wind-shear. This would be particularly useful for soaring in low wind speeds and large swell waves. Albatrosses probably use both wind shear and updrafts to gain kinetic energy, depending on the characteristics of the local wind and waves, but wind shear and dynamic soaring is thought to provide most of the energy for sustained soaring (Richardson, 2011).

The characteristics of the observed albatross flight were used to develop a simple model of dynamic soaring based on Rayleigh's (1883) concept of a bird soaring across a sharp wind-shear layer and on the aerodynamic equations of motion (Lissaman, 2005, 2007). The modeled flight pattern is referred to as the Rayleigh cycle since he was the first to describe the concept of dynamic soaring. The Rayleigh cycle, in which a bird circles across the boundary of two horizontal homogenous wind layers, is an efficient way to gain energy from a wind profile. The Rayleigh cycle predicts soaring airspeeds which agree well with more complex simulations of albatross flight (Lissaman, 2005; Richardson, 2011; Sachs, 2005).

Table 1. Minimum wind speed for dynamic soaring

	Wandering Albatross		Kinetic 100 Glider
Weight (pounds)	21		22.4
Wing Span (feet)	10		8.8
Maximum lift/drag	21.2		30
Cruise Speed (mph)	36		55
Loop Period (s)	Optimum: 7.2	Observed: 10	Optimum: 11.1
Minimum Wind Speed (mph)	7.5	7.9	8.1
Loop Diameter (feet)	121	167	286
Bank Angle (degrees)	54.7	45.7	54.7
Load Factor (g)	1.7	1.4	1.7

Minimum wind speed required for sustained dynamic soaring by a wandering albatross and a Kinetic 100 RC glider. The examples use the characteristics of a wandering albatross given by Pennycuick (2008) and a ballasted high-performance glider similar to a Kinetic 100, the present world speed record holder (http://www.dskinetic.com). Adding ballast (payload) to the 15 pound unballasted glider was assumed to maintain the same maximum lift/drag value and to increase the cruise airspeed, which corresponds to the maximum lift/drag value. Cruise speed is proportional to the square root of glider weight, and a 49% increase of glider weight increased cruise speed from 45 mph (unballasted glider) to 55 mph (ballasted glider). The minimum wind speed for energy-neutral dynamic soaring was calculated using the model Rayleigh cycle, the maximum lift/drag value for straight flight, the cruise airspeed, and the loop period. Loop diameter, bank angle and load factor were calculated using the loop period and cruise airspeed. Load factor is given in terms of the acceleration of gravity (g).

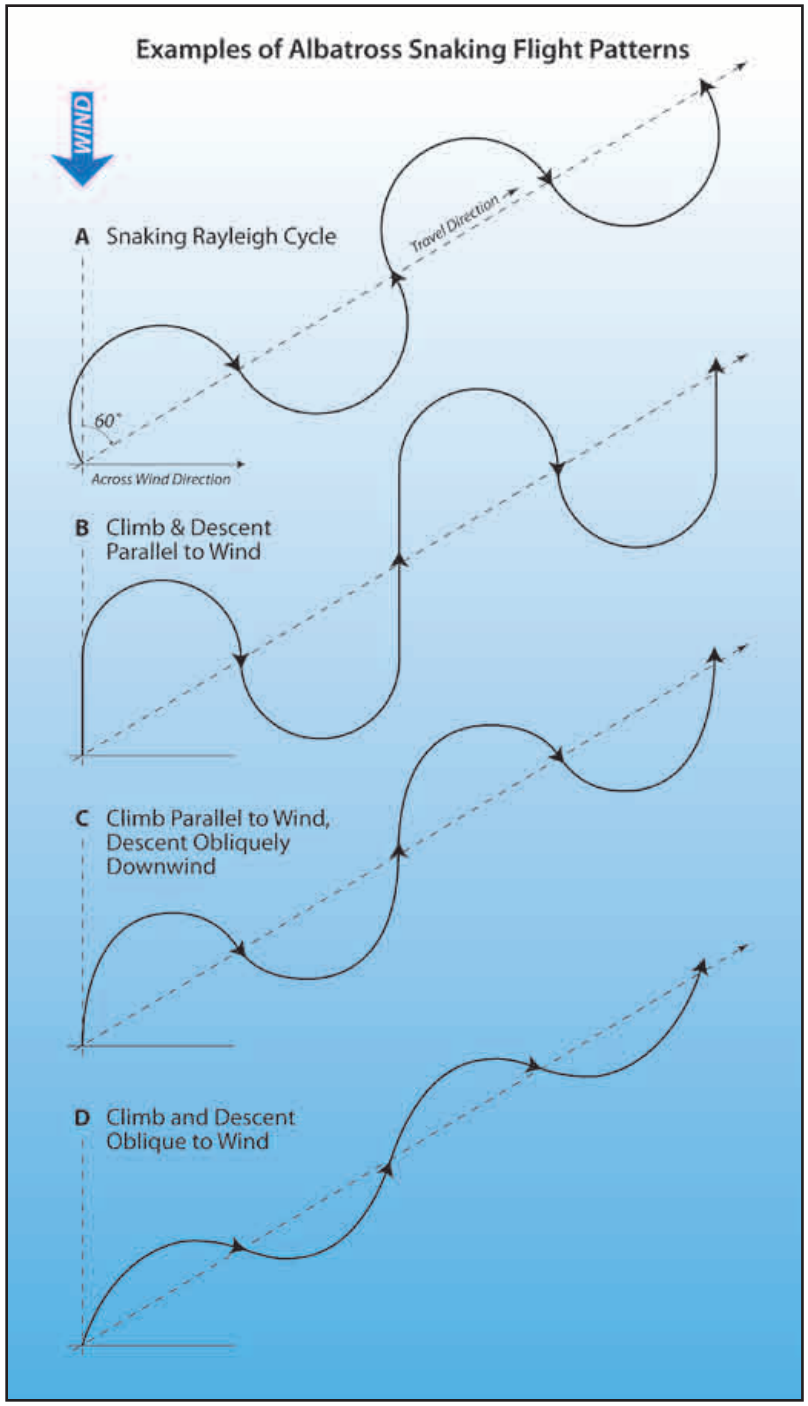

Figure 4. Plan view, showing examples of snaking (zigzag) flight at an angle of 60 degrees to the right of the wind similar to the flight shown in Figure 1. (A) Rayleigh snaking cycle created by linking together semi-circular pieces of the circular Rayleigh cycle to simulate the albatross zigzag flight pattern and average travel velocity. (B) Semi-circular snaking cycle modified to cross the wind-shear layer parallel to the wind direction for maximum energy gain. (C) Snaking cycle modified so that the upwind climb is parallel to the wind and the descent is obliquely downwind and parallel to wave crests; this pattern closely resembles my observations of albatross soaring and those of Idrac (1925, 1931). (D) Snaking cycle further smoothed so that the climb is obliquely upwind and the descent is mainly across-wind as observed by Idrac (1925, 1931). Flight patterns in panels C and D could be used to reduce energy gain in fast wind and large wind shear.

The essential assumptions are that an albatross soars in nearly-circular loops along a plane tilted upward into the wind and crossing the wind-shear layer with a small angle, so that vertical motions can be ignored. Vertical motions are ignored because no energy can be gained from them in a loop without wind. The sudden increase of airspeed (kinetic energy) caused by crossing the shear layer is assumed to balance the gradual loss of airspeed due to drag over half a loop, resulting in energy-neutral flight. Lift/drag values for the circular flight were modeled using the aerodynamic equations of motion for balanced circular flight (Lissaman, 2005, 2007; Torenbeek and Wittenberg, 2009) and a quadratic drag law, in which the drag coefficient is proportional to the lift coefficient squared. The derivations of the equations in the Rayleigh cycle model are given by Richardson (2011, 2012).

The Rayleigh cycle was used to estimate that a minimum wind speed of 7.5 mph is required for the sustained dynamic soaring of a wandering albatross. The minimum wind speed is a function of the loop period and albatross airspeed, and there is a minimum wind speed associated with an optimum loop period, which coincides with the minimum drag and energy loss in a loop. The absolute minimum wind speed occurs at an optimum loop period of 7.2 s and cruise airspeed of 36 mph (Table 1). The cruise airspeed is the airspeed at the maximum lift/drag value in straight flight. The 10 s observed typical loop period of a wandering albatross is somewhat larger than the optimum period and results in a slightly larger 7.9 mph minimum wind speed (Table 1). The larger 10 s loop period reduces the stall speed and load factor compared to values at the optimum loop period.

In low wind speeds some albatrosses and giant petrels are observed to alternate periods of flapping and gliding (flap-gliding) to assist dynamic soaring. When the wind completely dies, the birds often sit on the water surface. In calm conditions but with a large (~ 10 foot) swell running, albatrosses have been observed to soar without flap-gliding by using the updrafts over waves caused by the upward orbital motion of the wave surface (Alerstam et al., 1993; Froude, 1888; Pennycuick, 1982).

The travel velocity of a dynamic soaring albatross was modeled by dividing the Rayleigh cycle into semi-circular half loops and connecting a series of them together in a snaking flight pattern similar to that observed (Figure 4). The bird was assumed to quickly change banking directions during the upwind and downwind portions of its trajectory. The average travel velocity in flight perpendicular to the wind velocity was estimated to be 23 mph, based on the 36 mph cruise airspeed. The average travel velocity over the ground includes a downwind component due to leeway and is slower than 23 mph for a bird soaring upwind and faster when soaring downwind (Alerstam et al., 1993; Richardson, 2011; Wakefield et al., 2009). The simulations of albatross travel velocity using the Rayleigh cycle agree well with tracking measurements of real albatrosses soaring over the ocean.

3. Dynamic soaring of RC gliders

In April 2011, I watched pilots of radio-controlled (RC) gliders at Weldon Hill California use dynamic soaring to achieve glider speeds of up to 450 mph. The dynamic soaring at Weldon exploited the wind shear caused by fast wind blowing over a sharp-crested mountain ridge <http://www.rcspeeds.com>. Wind speed over Weldon Hill increased with height from near zero velocity at the ground level up to 50-70 mph as measured in gusts with an anemometer held overhead at a height of around 7 feet. The largest vertical gradient of wind velocity (largest wind shear) appeared to be located in a thin boundary layer located within several feet of the ridge crest. The fast wind blowing over the ridge formed an area of weaker wind or a lee eddy just downwind of the ridge crest and below the level of the crest. The wind-shear boundary layer was inferred to separate from the ridge

crest, to extend nearly horizontally in a downwind direction, and to gradually thicken with distance downwind.

The RC gliders flew in approximately circular loops lying roughly along a plane that tilted upward toward the wind direction, starting from the region in the lee of the ridge, extending above the ridge crest, and crossing the wind-shear layer near the ridge crest. The gliders flew in fast steeply-banked loops with a loop period of around 3 seconds. The glider wings looked like they were nearly perpendicular to the tilted plane all the way around a loop, implying very large accelerations. An accelerometer in a Kinetic 100 glider recorded a maximum acceleration of 90 g, the accelerometer's upper limit (Chris Bosley, personal communication). Glider speeds of 300-450 mph were measured with radar guns. Maximum measured glider speeds are around 10 times the wind speed, although this seems to be more realistic at lower speeds (< 350 mph) than at higher speeds (> 350 mph) (S. Lisenby, personal communication). The RC gliders had ailerons and an elevator to control flight and a fin in place of a moveable rudder. The ailerons and flaps could be adjusted to improve lift/drag during fast flight. Flaps reduced the stall speed when landing.

Maximum glider airspeeds in a Rayleigh cycle were calculated using optimum loop periods and also, for comparison, by using the relationship of glider speed equals 10 times wind speed (Figure 5). A typical high-performance RC glider like the present world speed record holder Kinetic 100 has a lift/drag value around 30, and the maximum possible dynamic soaring airspeed based on the Rayleigh cycle is around 9.5 times the wind speed of the upper layer. The model predicts that for wind speeds greater than around 10 mph the glider airspeed is proportional to values of maximum lift/drag and wind speed. This indicates that faster glider airspeeds could be achieved with gliders with larger values of maximum lift/drag. A key result is that over most of the range of wind speeds between around 10 mph and 30 mph (and higher) glider airspeed increases nearly linearly with wind speed from around 90 mph up to around 285 mph (Figure 5). This result appears to be in accord with the anecdotal observations of the very fast glider speeds as measured by radar guns.

The relationship between maximum glider airspeed and wind speed (Figure 5) is based on using the optimum loop period, which varies with glider speed as shown in Figure 6. As glider air speed and drag increase, the optimum loop period decreases to provide more frequent shear-layer crossings and to achieve energy-neutral flight. Optimum diameter, on the other hand, remains nearly constant at around 400 feet for airspeeds greater than around 120 mph (Figure 7). The typical period of fast glider loops at Weldon was around 3 s, although periods as small at 2 s are possible but difficult to fly in efficient dynamic soaring (C. Bosley and S. Lisenby, personal communications). The optimum loop period of 3 s occurs near an airspeed of 300 mph, suggesting that it is difficult to fly at optimum loop periods at glider speeds greater than around 300 mph (Figure 6). This suggests that higher wind speeds would be needed to achieve a particular airspeed than predicted by the curve in Figure 5 using the optimum loop period. Fast speeds and small loop periods cause large load factors ~ 30 g as shown in Figure 8.

The travel velocity of a dynamic soaring glider was modeled by dividing the Rayleigh cycle into semi-circular half loops and connecting a series of them together in a snaking flight pattern, similar to that of an albatross (Figure 4). The glider was assumed to quickly change banking directions during the upwind and downwind portions of its trajectory. The average travel velocity for flight perpendicular to the wind velocity was estimated to be around 6.1 times the wind speed (Figure 5). For example, a glider soaring in a wind of 20 knots (23 mph) from a favorable direction could fly with a travel velocity of 122 knots and

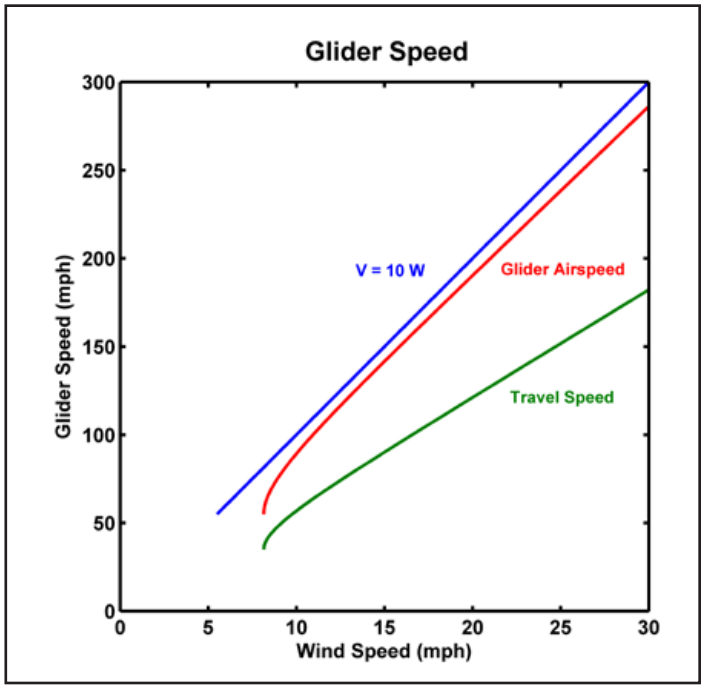

Figure 5. Maximum glider airspeed (red curve) calculated using a Rayleigh cycle and the optimum loop period, which coincides with the minimum energy loss in a loop and the maximum possible glider airspeed for a given wind speed. The value of maximum lift/drag in straight flight was assumed to equal 30 at the associated cruise airspeed of 55 mph (airspeed of minimum drag), values that are consistent with a Kinetic 100 RC glider with added ballast (payload) of around 50% of the unballasted glider weight. The blue straight line represents the relationship for which airspeed equals ten times the wind speed (V = 10 W) and assumes a maximum lift/drag value of 31.4. Travel speed (green curve) is the component of (average) travel velocity for flight perpendicular to the wind velocity, assuming a snaking flight pattern consisting of a series of semi-circular half loops (see Fig. 4).

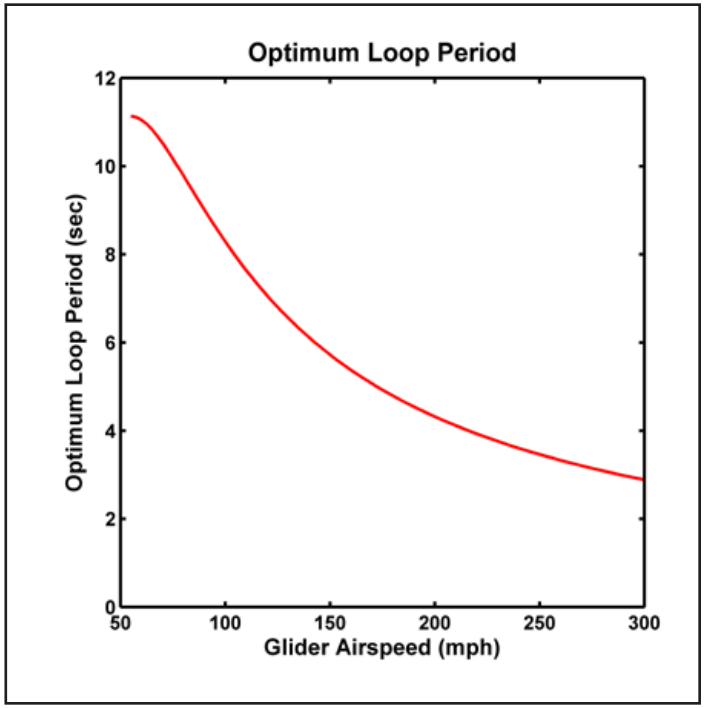

Figure 6. Optimum loop periods corresponding to the minimum energy loss in a loop and the maximum possible glider airspeeds in a Rayleigh cycle. The value of maximum lift/drag in straight flight was assumed to equal 30 at a cruise airspeed of 55 mph. Note that optimum loop periods decrease to around 3 s at an airspeed of 300 mph.

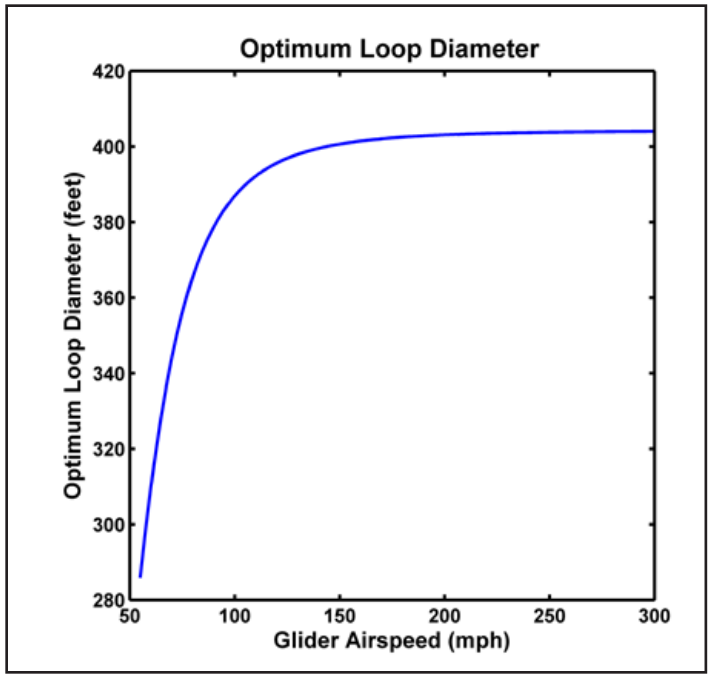

Figure 7. Optimum loop diameter corresponding to the optimum loop period and the associated maximum glider airspeed. Note that the loop diameter is approximately 400 feet for glider airspeeds greater than around 100 mph.

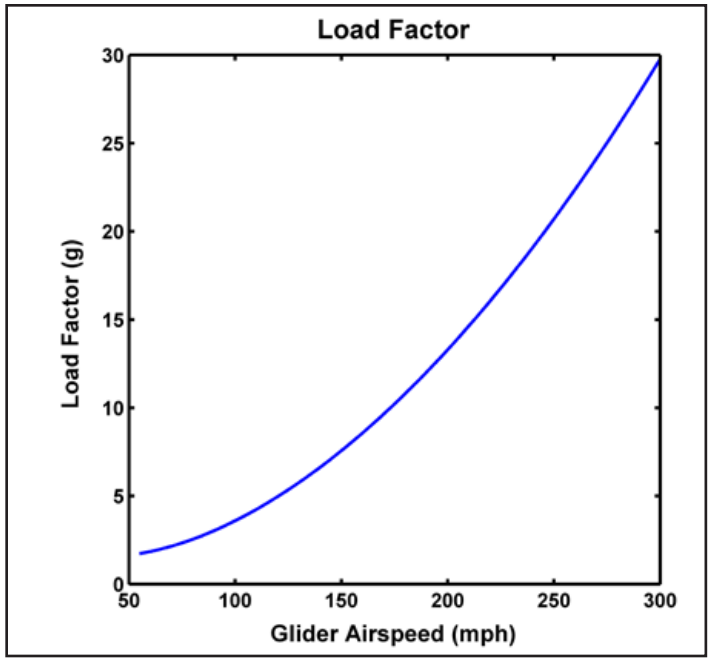

Figure 8. Load factor, which is the total acceleration of the glider in balanced circular flight, in terms of the acceleration of gravity (g). Load factor was calculated using the optimum loop period and glider airspeed. Note that values of load factor increase to around 30 times gravity at a glider airspeed of 300 mph. The corresponding bank angle is around 88 degrees.

cross the Atlantic in less than a day (from Woods Hole, MA to Brest, France, for example). Different travel velocities would be obtained in other directions relative to the wind, generally slower when headed into the wind and faster when headed downwind as was observed for albatrosses (see Deittert et al. 2009; Richardson 2011).

As in the case of an albatross, the Rayleigh cycle was used to estimate the minimum wind speed required for a high-performance glider to fly in energy-neutral dynamic soaring. Properties of a Kinetic 100 were used for the calculations, including an estimated maximum lift/drag value of 30 at a cruise speed of 55 mph (Table 1). The minimum wind speed is 8.1 mph at the glider airspeed of 55 mph, only slightly above the minimum wind speed (7.9 mph) for the wandering albatross. This airspeed of 55 mph corresponds to the glider's airspeed at the minimum sink rate in the loop, which is just above the stall speed. To help prevent a stall, the stall speed could be reduced by deploying flaps and also by increasing the loop period as in the case of a wandering albatross.

The 8 mph minimum wind speed for sustained dynamic soaring is small enough to suggest that it might not be fast enough to generate sufficiently large waves needed for gust soaring and that, therefore, gust soaring might

not be an appropriate model for such low winds. However, in the presence of decreasing winds, which had generated large waves, or in the presence of large swell propagating into an area from elsewhere, the waves might be sufficiently large enough with the addition of local wind waves to generate lee eddies, which could be used for gust soaring. Clearly, it would be beneficial to fly a dynamic-soaring UAV in regions of substantial winds and waves such as the Southern Ocean, home of most species of albatrosses, and the northern parts of the Atlantic and Pacific Oceans, especially during the windier times of the year. In low wind speeds a UAV could adapt techniques learned from the flight of albatrosses and exploit both updrafts over waves and supplemental power. Supplemental power could also assist take-off and landing. Numerical modeling of dynamic soaring in low winds and waves might help develop a successful strategy for these conditions.

4. Could a robotic albatross UAV use dynamic soaring to fly at high-speeds over the ocean?

In the low-level part of a swoop, an albatross flies very close to the ocean surface in a wave trough, close enough so that the bird's wing tip often grazes the water surface. This allows the bird to descend across the thin wind-shear layer and enter the lee eddy located in the wave trough and then turn and climb up across the thin wind-shear layer again. Grazing the surface of the water with wing-tip feathers does not appear to be a problem for an albatross, but touching the wing of a glider in the water could cause a crash. To avoid a crash, a UAV must maintain a safe gliding distance above the ocean surface. However, to fully exploit gust soaring through the thin wind-shear layer over waves, a UAV must also be able to descend down below the wind-shear layer into a wave trough, and this could be compromised if the minimum safe flying distance above the ocean surface were greater than the wave height. Therefore, it is possible that increasing a UAV height above the ocean for safety could lead to a reduced amount of energy being gained from the available wind shear (compared to an albatross and Rayleigh cycle) and a slower maximum airspeed, especially with low-amplitude waves.

A related issue is that optimum loop diameter of the glider in fast flight is around 400 feet, much larger than the 167 feet of a wandering albatross flying at an airspeed of 36 mph and loop period of 10 s (Table 1). The larger loop diameter could make it difficult to fully exploit the wind shear for maximum airspeed, since only the lower part of the loop would cross the wind-shear layer and the crossing could significantly deviate from a direction parallel to the wind as modeled by the Rayleigh cycle. Therefore, there is a question about whether the larger glider loop diameter would affect the exploitation of wind shear over waves and possibly lead to smaller maximum airspeeds than values predicted by the Rayleigh cycle.

In the snaking travel mode the bank angle changes twice in each loop period, where loop period used here means the period of two semi-circular half loops. The loop period of a wandering albatross is around 10 s, much larger than the fast ~ 3 s RC glider loops at a speed of 300 mph. This raises a question about whether a fast glider in a snaking flight pattern over the ocean could quickly alternate steep bank angles to the right and left with a loop period as small as 3 s. Some rapid high-speed acrobatic maneuvers performed at Weldon suggest that this would not be a problem, but fast snaking flight over ocean waves by a UAV needs to be demonstrated.

In order to explore these possible limitations to fast dynamic soaring over the ocean, it would be beneficial to have experienced pilots of RC gliders take high-performance (waterproof) gliders to sea and experiment with field trials in order to measure how fast dynamic soaring could be accomplished in realistic winds and waves. An RC glider flown from the shoreline or from a ship

would probably have to be confined to mainly short segments of snaking flight, to keep the glider in sight. In order to measure travel speed and further evaluate fast snaking flight, a car driving along the shore or possibly a helicopter might be used to track a fast glider. Perhaps a Coast Guard ship or helicopter could be made available, since a successful fast UAV glider could aid Coast Guard surveillance and search and rescue operations. In such demonstration flights it would be helpful to have instruments to measure high-resolution positions, orientations, velocities and accelerations over the ocean and through the air, as well as record detailed information about the wind and waves.

Deittert et al. (2009) discussed model simulations, which provide another evaluation of a UAV soaring flight over the ocean. They numerically modeled dynamic soaring over a flat ocean surface (no waves) using an exponential wind profile. Most (~ 65%) of the increase of wind speed above the (flat) ocean in their modeled 66-foot wind layer occurs in the first 3 feet, and thus most of the increase of wind speed of the wind profile was missed by their UAV because of its banked wings and the clearance to the water surface. Moderate glider speeds of 22-63 mph were obtained for a direction perpendicular to the wind direction in wind speeds of 18-45 mph (specified at a height of 66 feet). Their ratios of UAV travel speed to wind speed are around 1.6 as compared to 6.1 using the same wind speeds in the Rayleigh cycle as described above. Thus, gust soaring, which exploits the large wind shear located just downwind of ocean wave crests (and mountain ridges), is a more efficient way to obtain energy from the wind and to fly approximately four times faster than speeds achieved by using an exponential wind profile over a flat ocean. Simulations like those described by Deittert et al. could be made more relevant to soaring over the real ocean by incorporating the dynamic soaring of a UAV into models that resolve wind-wave interactions and features like lee eddies and detached shear layers, which albatrosses use for gust soaring. It seems probable that, when these features are incorporated into a simulation, a model UAV would fly closer to the speeds found using the Rayleigh cycle. Such simulations could also reveal information about optimal flight characteristics over waves. On the other hand, the slower travel speeds found by Deittert et al. could be more realistic in practice if UAV gust soaring turns out to be less efficient than predicted by the Rayleigh cycle.

5. Summary and conclusions

Fast dynamic soaring as demonstrated by RC gliders at Weldon CA was modeled in order to investigate the flight parameters that permit such fast flight and to evaluate whether dynamic soaring could be exploited by a robotic albatross UAV for fast flight over the ocean. A two-dimensional model (Rayleigh cycle) was developed of dynamic gust soaring along a plane that intersects a wind-shear layer. The model wind-shear layer is caused by a layer of uniform wind overlying a layer of zero wind, which was assumed to exist below and downwind of ocean wave crests and mountain ridge crests. The Rayleigh cycle was used to calculate the characteristics of energy-neutral dynamic soaring.

The maximum possible airspeed in the Rayleigh cycle coincides with the minimum energy loss in a loop and an optimum loop period. The optimum loop period was used to calculate the maximum glider speed as a function of wind speed. For wind speeds > 10 mph and a typical glider maximum lift/drag value of around 30, the maximum glider airspeed was found to equal around 9.5 times the wind speed in the upper layer. Both the fast measured RC glider speeds at Weldon and the results of the model Rayleigh cycle indicate how effective gust soaring through a wind-shear layer can be for extracting energy and using it to fly at exceptionally fast speeds. Maximum (average) travel velocity perpendicular to the wind velocity using the Rayleigh cycle in a snaking flight

pattern similar to that of an albatross was found to be around 6.1 times the wind speed.

Could dynamic soaring be used by a UAV for high-speed flight over the ocean? As long as sufficiently fast winds and large waves generate lee eddies and the strong shear layers located above them, then in principle dynamic gust soaring could be used for high-speed flight. This assumes a snaking flight pattern similar to that of an albatross. However, for safety, a UAV needs to maintain a larger clearance above the water surface than does an albatross, which suggests that field experiments need to be performed to investigate how well a UAV can fully exploit the wind-shear layer above wave troughs to fly at fast speeds. In addition there are questions about how the larger optimum diameter and smaller optimum loop period of fast flight in the Rayleigh cycle could affect fast flight in practice. Test flying RC gliders at sea in various wind and wave conditions would be a good way to assess fast dynamic soaring over the ocean, especially the snaking travel mode of flight.

To further investigate the dynamic soaring of gliders over the ocean, it would be helpful to add instruments to measure high-resolution positions, orientations, velocities and accelerations over the ground and through the air, as well as information about the structure of the wind interacting with waves. Numerical modeling could be used to investigate high-speed dynamic gust soaring over ocean waves and help refine high-performance glider design and optimum flight patterns. A robotic albatross UAV would require the ability to measure and respond to the topography of the ocean surface (waves crests and troughs), the adjacent wind field, and obstructions like ships. Back-up power would be needed to help launch and recover a UAV and for low wind conditions, when dynamic soaring plus wave-slope soaring could be insufficient for energy-neutral soaring. Given sufficient wind, energy from dynamic soaring could be used to provide power for an autopilot, instrumentation, navigation, communication and an auxiliary motor. This would result in a somewhat slower UAV compared to the maximum speed possible but would be acceptable for many applications.

Acknowledgements.

I profited from discussions with Peter Lissaman about the aerodynamics of gliding flight and the model Rayleigh cycle. Chris Bosley and Spencer Lisenby invited me to see fast dynamic soaring at Weldon Hill CA and explained and discussed RC glider dynamic soaring techniques. Don Herzog flew me down to Bakersfield in his high-performance Trinidad airplane at 200 mph (much slower than the RC gliders) and joined in the trip up to Weldon. Paul Oberlander helped draft some of the figures.

References

Alerstam, T., Gudmundsson, G. A., Larsson, B., 1993. Flight tracks and speeds of Antarctic and Atlantic seabirds: radar and optical measurements. Philosophical transactions of the Royal Society of London B 340, 55-67.

Deittert, M., A. Richards, C. A. Toomer, A. Pipe, 2009: Engineless UAV propulsion by dynamic soaring, Journal of Guidance, Control, and Dynamics, 32 (5), 1446-1457.

Froude, W., 1888. On the soaring of birds. Proceedings of the Royal Society of Edinburgh 15, 256-258.

Gent, P. R., Taylor, P. A., 1977. A note on “separation” over short wind waves. Boundary-Layer Meteorology 11, 65-87.

Hristov, T. S., Miller, S. D., Friehe, C. A., 2003. Dynamical coupling of wind and ocean waves through wave-induced air flow. Nature, 422, 55-58.

Hsu, C.-T., Hsu, E. Y., Street, R. L., 1981. On the structure of turbulent flow over a progressive water wave: theory and experiment in a transformed, wave-

following co-ordinate system. Journal of Fluid Mechnanics 105, 87-117.

Idrac, P., 1925. Étude expérimentale et analytique du vol sans battements des oiseaux voiliers des mers australes, de l'Albatros en particulier. La Technique Aeronautique 16, 9-22.

Idrac, P., 1931. Études expérimentales sur le vol à voile au lieu même d'évolution des grands oiseaux voiliers (vauturs, albatros, etc.); son application au vol à voile humain. Vivien, Paris, pp. 75.

Kawai, S., 1982. Structure of air flow separation over wind wave crests. Boundary-Layer Meteorology 23, 503-521.

Lissaman, P., 2005. Wind energy extraction by birds and flight vehicles. American Institute of Aeronautics and Astronautics Paper 2005-241, January 2005.

Lissaman, P., 2007. Fundamentals of energy extraction from natural winds. Technical Soaring 31(2), 36-41.

Pennycuick, C. J., 1982. The flight of petrels and albatrosses (Procellariiformes), observed in South Georgia and its vicinity. Philosophical Transactions of the Royal Society of London B 300, 75-106.

Pennycuick, C. J., 2002. Gust soaring as a basis for the flight of petrels and albatrosses (Procellariiformes). Avian Science 2, 1-12.

Pennycuick, C. J., 2008. Modelling the flying bird. Academic Press, New York, pp. 496.

Rayleigh, J. W. S., 1883. The soaring of birds. Nature 27, 534-535.

Reul, N., Branger, H., Giovanangeli, J.-P., 1999. Air flow separation over unsteady breaking waves. Physics of Fluids 11(7), 1959-1961.

Richardson, P. L., 2011: How do albatrosses fly around the world without flapping their wings? Progress in Oceanography 88, 46-58.

Richardson P. L., 2012: High-speed dynamic soaring. Radio-Controlled Soaring Digest, April 2012, 29 (4), 36-49.

Sachs, G., 2005. Minimum shear wind strength required for dynamic soaring of albatrosses. Ibis 147, 1-10.

Sullivan, P. P., Edson, J. B., Hristov, R., McWilliams, J. C., 2008. Large-eddy simulations and observations of atmospheric marine boundary layers above non-equilibrium surface waves. Journal of the Atmospheric Sciences 65, 1125-1245.

Sullivan, P. P., McWilliams, J. C., Moeng, C.-H., 2000. Simulations of turbulent flow over idealized water waves. Journal of Fluid Mechanics 404, 47-85.

Torenbeek, E., Wittenberg, H., 2009. Flight Physics: Essentials of Aeronautical Disciplines and Technology, with Historical Notes. Springer, New York, pp. 535.

Wakefield, E. D., Phillips, R. A., Matthiopoulos, J., Fukuda, A., Higuchi, H., Marshall, G. J., Trathan, P. N., 2009. Wind field and sex constrain the flight speeds of central-place foraging albatrosses. Ecological Monographs 79, 663-679.